MSDE

PAPER

View Article Online
View Journal | View Issue

Cite this: *Mol. Syst. Des. Eng.*, 2021, **6**, 390

Naturally occurring polyphenols as building blocks for supramolecular liquid crystals – substitution pattern dominates mesomorphism†

Jan Balszuweit,‡[a] Meik Blanke,‡[a] Marco Saccone,[ab] Markus Mezger,[cd] Constantin G. Daniliuc,[e] Christoph Wölper,[f] Michael Giese *[a] and Jens Voskuhl *[a]

Received 23rd December 2020,
Accepted 9th March 2021

DOI: 10.1039/d0me00171f

rsc.li/molecular-engineering

A modular supramolecular approach towards hydrogen-bonded liquid crystalline assemblies based on naturally occurring polyphenols is reported. The combination of experimental observations, crystallographic studies and semi-empirical analyses of the assemblies provides insight into the structure–property relationships of these materials. Here a direct correlation of the number of donor OH-groups as well as their orientation with the mesomorphic behavior is reported. We discovered that the number and orientation of the OH-groups have a stronger influence on the mesomorphic behavior of the supramolecular assemblies than the connectivity (*e.g.* stilbenoid or chalconoid) of the hydrogen bond donors. Furthermore, the photo-switching behavior of selected complexes containing azopyridine ligands was investigated. This study will help future scientists to gain a deeper understanding of the underlying mechanisms and structure–property relationships of supramolecular assemblies with mesomorphic behavior, which is still one of the major challenges in current science.

Design, System, Application

We investigated hydrogen-bonded assemblies (HBAs), consisting of naturally occurring polyphenols (HB donors) and alkylated stilbazoles (St) and azopyridines (Ap) (HB acceptors), concerning their liquid crystalline properties. To this end five different phenols, namely butein, isoliquiritigenin, resveratrol, piceatannol and oxyresveratrol, were assembled with St or Ap in all possible ratios yielding 36 HBAs, which were analyzed in detail using infrared spectroscopy, polarized optical microscopy, differential scanning calorimetry and small and wide angle X-ray scattering. We discovered mainly nematic phases for the complexes, whereas it is noteworthy that only the 1 : 3 complexes melted homogeneously leading to the assumption that this stoichiometry is favored for all complexes, which can be attributed to the substitution pattern of the phenols. Only oxyresveratrol reveals smectic behavior as a 1 : 3 complex and a nematic mesophase as a 1 : 4 complex. Additionally we discovered that the connectivity, chalconoid or stilbenoid, is less important for the mesomorphism than the substitution pattern of the phenols. This in-depth structure–property relationship of naturally occurring polyphenols will be appealing to a broader readership, since prediction of mesomorphic behavior is still challenging. We are sure that our study will help to gain a deeper understanding of the underlying principles in HBAs with liquid crystalline properties.

[a] *Faculty of Chemistry (Organic Chemistry) and CENIDE, University of Duisburg Essen, Universitätsstraße 7, Essen 45141, Germany.*
E-mail: michael.giese@uni-due.de, jens.voskuhl@uni-due.de
[b] *Dipartimento di Ingegneria, Università degli Studi di Palermo, Viale delle Scienze 6, 90128 Palermo, Italy*
[c] *Faculty of Physics, University of Vienna, Boltzmanngasse 5, 1090 Vienna, Austria*
[d] *Max Planck Institute for Polymer Research, Ackermannweg 10, 55128 Mainz, Germany*
[e] *Organisch-Chemisches Institut, Westfälische Wilhelms Universität Münster, Corrensstraße 40, 48149 Münster, Germany*
[f] *Faculty of Chemistry (Inorganic Chemistry) and CENIDE, University of Duisburg-Essen, Universitätsstrasse 7, 45117 Essen, Germany*

† Electronic supplementary information (ESI) available: Additional DSC, POM and IR measurements as well as information on the Hirshfeld calculations. CCDC **Pic(Ap$_8$)$_3$** (1945777) and **Pic(St$_8$)$_3$** (1942435). For ESI and crystallographic data in CIF or other electronic format see DOI: 10.1039/d0me00171f

‡ The two authors contributed equally to this work.

Introduction

Nature is an inexhaustible source of chemical precursors, drugs,[1] and materials.[2] Particularly in the context of green and sustainable chemistry, naturally occurring compounds have become the focus of recent research for the fabrication of functional materials such as polymers,[3] (hydro)-gels[4] and nanoparticles.[5] One of the first nature-inspired examples of a well-known class of materials – liquid crystals – was found for cholesterol derivatives back in the year 1889, when Reinitzer discovered an unusual behavior for this compound showing an unknown aggregate state between liquid and crystalline at elevated temperature, which showed birefringence.[6] Ever since, liquid crystalline materials have been studied intensively by research groups all over the

world. In this regard, several approaches to obtain liquid crystalline materials have been investigated. The classic approach consists of the synthesis of mesogens such as biphenyls and more sophisticated molecules, containing an aromatic core unit which is functionalized with hydrocarbons or fluorocarbons.[7] This synthetic approach suffers from several problems, such as long synthetic routes, expensive starting materials and inflexibility, which can be overcome by a supramolecular approach. Supramolecular chemistry provides an efficient approach towards the fabrication of functional materials by employing non-covalent interactions. Simple mixing of pre-tailored molecular building blocks provides access to a variety of functional materials by self-assembly and allows manipulation of the properties by variation of the components without the need for additional syntheses. In particular hydrogen- and halogen-bonded liquid crystals have been studied intensively by several groups in the past few years.[8]

Although a huge number of such systems have been reported, the complexity of the interplay of non-covalent interactions as well as their careful orchestration is still challenging and remains unpredictable over wide areas. Hence, stepwise variation of the structures remains the only way to gain deeper insights into the structure–property relationship of supramolecular liquid crystalline assemblies.

Recently Giese and co-workers established a modular approach towards hydrogen-bonded liquid crystalline materials with photo-responsive behavior by introducing alkylated azopyridine (**Ap**) or stilbazole (**St**) units as hydrogen acceptors and aromatic phenols such as phloroglucinol, resorcinol, hydroquinone and resveratrol (**Res**) as hydrogen donors.[9] The latter, furthermore, responds to UV-light irradiation (300 nm) by undergoing photo-cyclisation to resveratrone, leading to a change in the mesophase.[10] In this contribution, we expanded our scope to four additional, naturally occurring stilbenoids and chalconoids namely oxyresveratrol (**Oxy**), piceatannol (**Pic**), butein (**But**) and isoliquiritigenin (**Iso**) as hydrogen bond donors in combination with octyl-chain containing azopyridine ($\mathbf{Ap_8}$) and stilbazole ($\mathbf{St_8}$) as hydrogen bond acceptors (Fig. 1). Herein we report a systematic study on the structure–property relationship of hydrogen-bonded liquid crystals based on stilbenoids and chalconoids. Thereby, we focus on four aspects affecting the mesomorphic behavior: the role of the ratio of the hydrogen bond donor and acceptor, the influence of the hydrogen bond accepting moiety, the impact of the number and relative position of the OH-groups in the hydrogen bond donors and the role of the linking group of the hydrogen bond donating moiety.

Hydrogen-bonded mesogens were obtained by simple mixing of the acceptors and the donors, yielding a library of hydrogen-bonded assemblies, which were analyzed with respect to their mesomorphic behavior. Furthermore, computational analyses, small- and wide-angle X-ray scattering (SAXS, WAXS) and single X-ray diffraction analyses were performed to support the obtained findings for the mesomorphism.

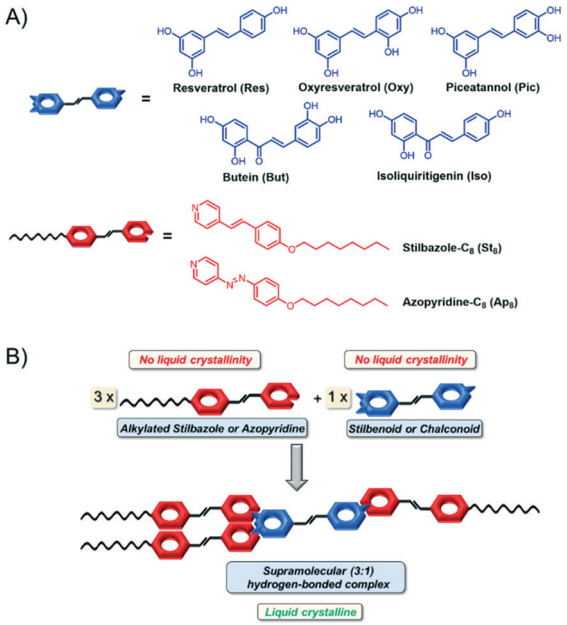

Fig. 1 A) Molecular structures of the investigated stilbenoids and chalconoids (hydrogen donors, blue) as well as the alkylated stilbazoles and azopyridines (hydrogen acceptors, red). B) Schematic presentation of the modular approach towards hydrogen-bonded liquid crystalline assemblies with stilbenoids or chalconoids as core units.

Results and discussion

Formation of the hydrogen-bonded assemblies (HBAs)

The hydrogen-bonded assemblies (HBAs) were obtained by mixing acetonic solutions of the hydrogen bond donors (**Res**, **Oxy**, **Pic**, **But**, **Iso**) with the corresponding hydrogen bond acceptors ($\mathbf{St_8}$, $\mathbf{Ap_8}$, Fig. 1) in ratios of 1 : 4, 1 : 3, 1 : 2 and 1 : 1. By slow evaporation of the solvent a series of 36 hydrogen-bonded assemblies were obtained. To prove the formation of the hydrogen-bonded assemblies, IR spectroscopy was performed (ESI,† Fig. S1). Taking the $\mathbf{Oxy(St_8)_3}$ assembly as a representative example, a shift of the OH vibration of oxyresveratrol upon formation of the HB assembly is observable. In addition to the shift of the OH band from ~3170 cm^{-1} to ~3060 cm^{-1}, a sharpening and loss of intensity for this band can be observed. Furthermore, the band at 2650 cm^{-1} indicates the N–H interaction between the donor and acceptor moieties. This behavior can be observed for every HB assembly investigated in the present study (ESI,† Fig. S1). Since neither the hydrogen bond donating nor the accepting moiety shows LC properties prior to assembly formation, a further proof for the formation of the HBAs is given by the induction of liquid crystallinity. A summary of the mesogenic properties of the 1 : 3 complexes is given in Fig. 2.

Role of the ratio of the hydrogen bond donor : acceptor

Initial polarized optical microscopy (POM) studies revealed that complexes in the ratios of 1 : 1, 1 : 2 and 1 : 4 showed inhomogeneous melting behavior which was attributed either

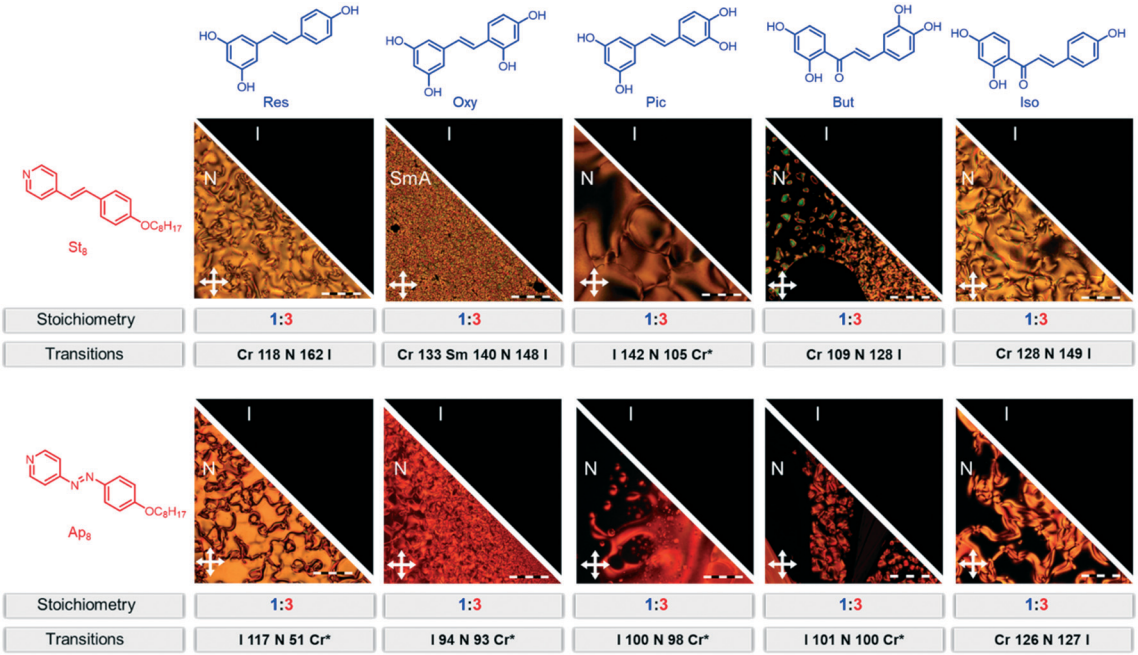

Fig. 2 Summary of all hydrogen-bonded assemblies in the present study. Given are the transitions and transition temperatures as determined by POM with a heating and cooling rate of 10 °C min^{-1} (temperatures are given in °C). Transitions marked with * are monotropic and occur only on cooling. The scale bar represents 100 μm. The data of **Res(St$_8$)$_3$** and **Res(Ap$_8$)$_3$** have been reported before and are shown for comparative reasons.[10]

to free hydrogen bond donors or acceptors. For instance the POM and DSC data of the 1 : 4 mixtures of **Pic** and **But**, which contain in total four hydroxy-groups, showed two melting points, one for the 1 : 3 assembly and one additional which corresponds to the free hydrogen bond acceptors (**St$_8$** or **Ap$_8$**) (Fig. S48–S63†). For the 1 : 4 complexes we additionally observed homogeneous melting for **Oxy(St$_8$)$_4$** and **Oxy(Ap$_8$)$_4$** (see ESI† Fig. S40 and S44). In contrast, all 1 : 3 assemblies show homogeneous melting behavior and defined phase transitions. We attribute this observation to the partial blocking of the hydrogen bond donors by inter- or intramolecular hydrogen bonding.[11] Therefore, the following discussion focuses mainly on the 1 : 3 assemblies. Our hypothesis is supported by X-ray crystallography, which revealed the desired 1 : 3 complex between **Pic** and **St$_8$** even if a 1 : 2 ratio is used. This indicates that the formation of the 1 : 3 complex is favoured in the solid state (see the Description of the crystal structures section) which is in line with the phase separation and inhomogeneous melting of the 1 : 1 and 1 : 2 complexes. The influence of intra- and intermolecular hydrogen bonds on the complex stoichiometry will be discussed in detail in the following section (*vide infra*).

Influence of the hydrogen bond accepting moiety

The nature of the hydrogen bond accepting moiety, namely **St** or **Ap**, has a crucial impact on the temperature range of the mesophase and meting points of the assemblies. It is furthermore obvious that the stilbenoid complexes with **Ap$_8$** as well as the **Ap$_8$** complexes of the chalconoids show narrower temperature ranges than the comparable **St$_8$** complexes which could also be attributed to the higher tendency of **Ap** to crystallize (Fig. S2†). This observation is in agreement with the literature, showing that **Ap** is an inferior promesogen when compared to **St**.[12] This observation can be attributed to the repulsion of the free electron pairs on the azo-linking group, destabilizing the mesophase of the corresponding assemblies.[9a] Since the results of the present study indicate very narrow temperature ranges for the liquid crystalline states of the **Ap** moieties, the following discussion will mainly focus on the results obtained for the stilbazole-based assemblies. **Ap** is nonetheless able to be switched from the *trans* to the *cis* state under UV-light irradiation (λ_{ex} = 365 nm), which will be discussed in the "Photo-responsiveness of the HBAs" section (*vide infra*).

Impact of the number and relative position of the hydroxy-groups in the hydrogen bond donors

Obviously, the relative position of the hydroxy-groups plays a significant role in the mesomorphic properties. *ortho*-Positioned hydroxyl groups led to intramolecular hydrogen bonding, blocking one hydrogen bond donating moiety, as observed in the X-ray structure of the **Pic** complexes with **Ap$_8$** and **St$_8$** (*vide infra*). Furthermore, we found intermolecular hydrogen bonding of the remaining free OH-groups with adjacent **Pic** leading to the observed packing in the crystal lattice. To gain a deeper understanding of the intra- and intermolecular hydrogen bonding of the

pure stilbenoids and chalconoids **Pic**, **Iso** and **But** which feature either *ortho* positioned OH-groups (**Pic**), a chalcone moiety (**Iso**) or both (**But**), we investigated their packing in the crystal lattice. In the crystal structure of **Pic**[13] (CCDC 706345) (Fig. S66†) intermolecular hydrogen bonding was observed for one of the *ortho* positioned hydroxy-groups which is in accordance to the X-ray structure of the $\mathbf{Ap_8}$ and $\mathbf{St_8}$ complexes (*vide infra*). This behavior supports the preference for the 1 : 3 complexes, since one hydroxy-group participates in the packing in the crystal lattice and hence is unable to form a hydrogen bond with a hydrogen acceptor moiety. **But**[14] (CCDC 1117309) and **Iso**[15] (CCDC 916410), furthermore, feature intramolecular hydrogen bonds between the carbonyl-group and the adjacent hydroxy-group which can be observed in the crystal structure of the pure hydrogen bond donors, which have been described before (Fig. S67 and S68†).[14,15] We noticed that, although this hydrogen bond is present in the structure of the pure compounds, the hydroxy-group participated in the HBA due to homogeneous melting of the **Iso** 1 : 3 complexes. Furthermore, the observations of **Pic** concerning *ortho*-positioned OH groups also apply for **But**, since homogeneous melting was only observed for the 1 : 3 complex and not for the 1 : 4 assemblies.

Role of the linking group of hydrogen bond donors

In this paragraph we aim for a direct comparison of the used stilbenoids to gain a deeper understanding of the structure–property relationship. The stilbenoids **Res**, **Oxy** and **Pic** differ exclusively in their hydroxyl substitution pattern on the second benzene unit whereas the other aromatic unit features two hydroxyl-groups in the *meta* position (Fig. 1). As already reported, $\mathbf{Res(St_8/Ap_8)}$ showed a nematic liquid crystalline phase with the typical "Schlieren" texture (Fig. 3 and ESI† Fig. S5 and S6).[10] Here it was found that **Pic** is comparable with **Res** since only nematic structures were found for the 1 : 3 complexes with $\mathbf{St_8}$ and $\mathbf{Ap_8}$ (see Fig. 2 and 3).

Comparing the $\mathbf{Pic(Ap_8)_3}$ assembly with the corresponding $\mathbf{Res(Ap_8)_3}$ assembly reveals a monotropic and very narrow temperature range of 2 °C of the nematic phase with simultaneous crystallization. Also in the case of the $\mathbf{Pic(St_8)_3}$ assembly a drastic decrease in the temperature range of the mesophase was observed. In both cases the narrow temperature range of the mesophase is related to a significantly increased crystallization temperature. These findings were attributed to the fact that one vicinal OH group remains free and thus, does not bind to the hydrogen bond acceptor. However, in the densely packed crystalline phase, this free OH group interacts with neighbouring assemblies promoting the crystallization of the assemblies.[13] This assumption is supported by single crystal X-ray diffraction analyses. For all donor : acceptor ratios (*e.g.* 1 : 3 and 1 : 4) only suitable crystals of the 1 : 3 complexes were obtained (see description of the crystal structures subchapter, *vide infra*). Interestingly, only $\mathbf{Oxy(St_8)_3}$ shows a transition from the nematic (ΔT_N = 23 °C) into a smectic phase (ΔT_{SmA} = 48 °C). Upon cooling of the $\mathbf{Oxy(St_8)_3}$ complex, first the "Schlieren" texture is observed, which undergoes a transition into a pseudo focal-conic texture (Fig. 2 and 3 and ESI† Fig. S9). The transition from the nematic to a smectic phase was confirmed by small angle X-ray scattering (SAXS) (Fig. 4 and S64 and S65†). Analysis of the radial averaged scattering patterns on the smectic mesophase reveals a periodicity of 4.3 nm and 0.45 nm for the long and short axis, respectively. The temperature range, in which the liquid-crystalline phase appears, is also significantly higher for **Oxy** (ΔT = 72 °C for $\mathbf{St_8}$) than for **Pic** (Fig. 2 and 3), which we attribute to the missing interference of intra- *versus* intermolecular hydrogen bonding for the **Oxy**-based assemblies. The 1 : 4 complexes of **Oxy** with **Ap** and **St** revealed only nematic behavior. To sum up, all three $\mathbf{St_8}$ complexes reveal mesomorphism over a broad temperature range revealing nematic (**Res** and **Pic**) or smectic (**Oxy**) phases.

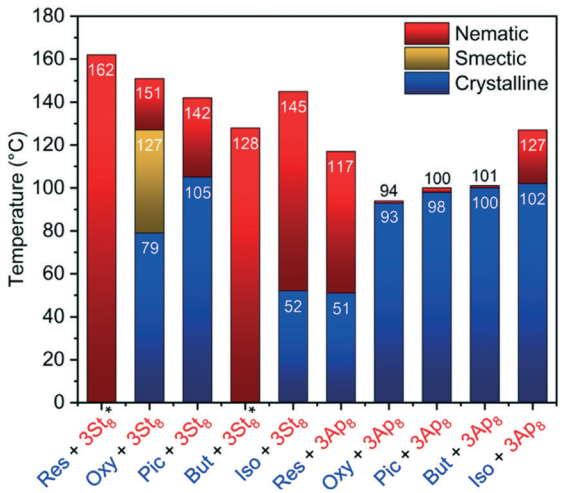

Fig. 3 Summary of the LC properties of the 1 : 3 complexes reported in the present study, measured on cooling with a rate of 10 °C min^{-1} under a POM. Clearing points are reported and complexes marked with * undergo a transition into a glassy state, preserving the texture of the liquid crystalline phase (temperatures are given in °C). The data of $\mathbf{Res(St_8)_3}$ and $\mathbf{Res(Ap_8)_3}$ have been reported before and are shown for comparative reasons.[10]

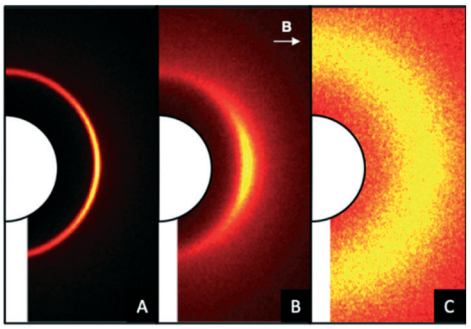

Fig. 4 SAXS patterns of $\mathbf{Oxy(St_8)_3}$ in a smectic (A), nematic (B) and isotropic (C) phase. The nematic phase (B) was oriented by a horizontal magnetic field B (arrow).

Besides stilbenoids, the liquid crystalline properties of the chalconoid HBAs of **But** and **Iso** were investigated, showing the characteristic "Schlieren" texture of a nematic phase for all assemblies. **But** and **Iso** reveal the same substitution pattern of the hydroxyl-groups like **Pic** and **Res** respectively, but differ in the linkage between the two arene moieties featuring a carbonyl group (chalcone backbone). It is noticeable that **Iso(St$_8$)$_3$** forms an enantiotropic mesophase with a broad temperature range upon cooling (ΔT_N = 93 °C), whereas **But(St$_8$)$_3$** shows monotropic phase behavior with the formation of a glassy state preserving the nematic mesophase (Fig. 3 and ESI† Fig. S21–S27). The additional free vicinal hydroxy-group of **But** seems to broaden the temperature range of the liquid crystalline state in the **St**-complex and thus prevents the crystallization on cooling. However, if the **Ap** complexes of the two compounds are considered, the **Iso**-complex has a much broader temperature range of the nematic phase as its substitution pattern is comparable with that of **Res**, featuring a single hydroxy-group *para*-oriented to the double bond bridge.

Photo-responsiveness of the HBAs

If azopyridine is used as the hydrogen bonding acceptor, it allows for reversible photo-switching.[9a] Due to irradiation with UV-light (405 nm) reversible *trans–cis* isomerization is induced, which leads to a structural change, followed by a transition from the nematic to the isotropic state. Irradiating the complex **Iso(Ap$_8$)$_3$** in its mesophase at 110 °C, using a commercially available laser pointer (5 mW) with a wavelength of 405 nm, a transition from the nematic to the isotropic state can be induced (Fig. 5). Before irradiating the sample the typical "Schlieren" texture of the nematic phase can be observed. After irradiation, with a wavelength of 405 nm, this texture vanishes and no birefringence is present, indicating the isotropic state. This transition can be attributed to the reversible *trans–cis* switching of the azo-compounds, which changes the shape of the molecule and therefore disturbs the orientation of the calamitic liquid crystals due to the bent shape.

This photo-switching is reversible and after removal of the UV light the "Schlieren" texture reappears within less than a second, which was reproduced for several cycles. A similar behavior was observed for **Pic(Ap$_8$)$_3$** (Fig. 5) showing that this photo-isomerization is independent from the connectivity of the HB donors using either stilbenoids or chalconoids.

Description of the crystal structures

For two hydrogen-bonded assemblies the formation of the assembly was additionally confirmed by X-ray diffraction analysis of single crystals. The complex **Pic(Ap$_8$)$_3$** crystallizes in the centrosymmetric space group $P2_1/n$ with four molecules in the unit cell. The solid-state structure clearly shows the formation of hydrogen bonds between **Pic** and **Ap$_8$** (OH$\cdots$N$_{py}$ = 1.823, 1.912, 1.935 Å, O$\cdots$N$_{py}$ = 2.722, 2.761 and 2.755 Å, Fig. 6).

Pic was found to be disordered over two positions in the asymmetric unit. In the packing diagram a linear chain along the *c*-axis involving auxiliary hydrogen bond interactions between two adjacent piceatannol molecules (OH$\cdots$O = 1.950 Å) and $\pi\cdots\pi$ interactions between pyridine–pyridine rings (3.348 Å; 3.352 Å) and phenyl–phenyl rings (3.375 Å, 3.388 Å) was formed (Fig. 6C). The 3D network is furthermore supported by numerous additional CH$\cdots\pi$ and $\pi\cdots\pi$ interactions. Replacing the azopyridine acceptor unit with **St$_8$** yielded the related solid state structure of **Pic(St$_8$)$_3$**. The three hydrogen bonds between the hydroxy-groups of the piceatannol and the pyridine nitrogen atom of stibazole-C$_8$ are OH$\cdots$N$_{py}$ = 1.769, 1.811, and 1.831 Å (O$\cdots$N$_{py}$ = 2.691, 2.758 and 2.696 Å, Fig. 7A), respectively. These hydrogen bonds are slightly shorter compared to those found in the complex **Pic(Ap$_8$)$_3$**. In contrast to the linear chain found in the packing diagram of **Pic(Ap$_8$)$_3$**, which presents an alternating orientation of the **Pic** moiety, the solid state packing of **Pic(St$_8$)$_3$** shows a parallel orientation of the **Pic**

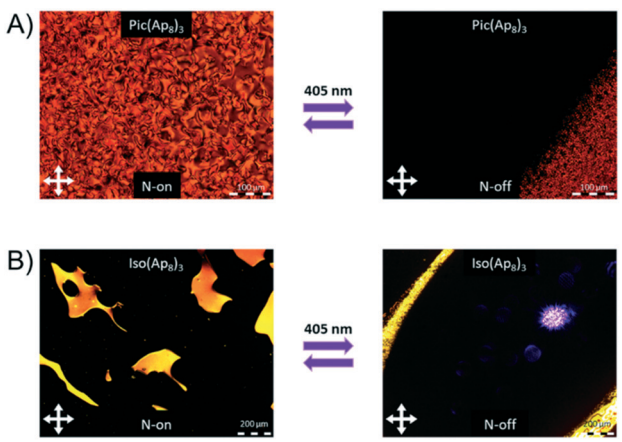

Fig. 5 POM images showing the photo-switchability of the nematic phase of A) **Pic(Ap$_8$)$_3$** at 105 °C and B) **Iso(Ap$_8$)$_3$** at 110 °C with a wavelength of 405 nm.

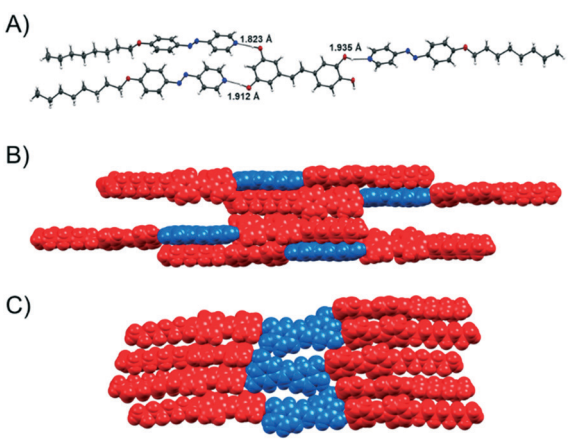

Fig. 6 A) X-ray structure of the 3 : 1 **Pic(Ap$_8$)$_3$** assembly; B) space filling model of the packing in side view and C) in top view. Colored in red: azopyridine (**Ap$_8$**), colored in blue: piceatannol (**Pic**).

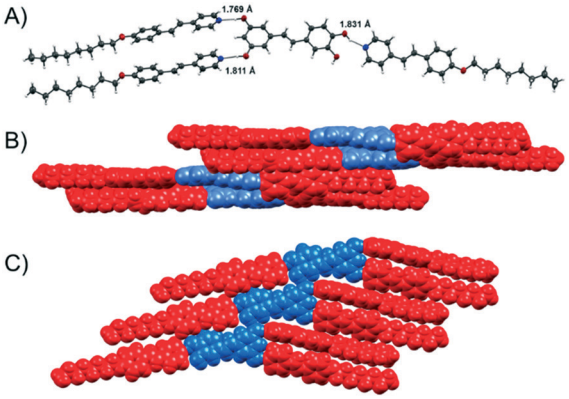

Fig. 7 A) X-ray structure of the 3 : 1 supramolecular hydrogen-bonded **Pic(St$_8$)$_3$** complex; B) space filling model of the packing in side view and C) in top view. Colored in red: stilbazole (**St$_8$**), colored in blue: piceatannol (**Pic**).

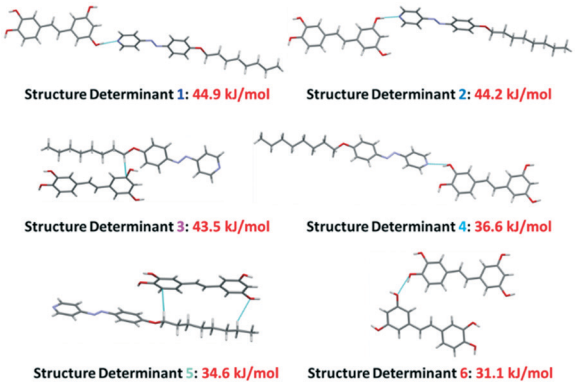

Fig. 8 Supramolecular hierarchy of the six most stabilizing interactions in the **Pic(Ap$_8$)$_3$** structure as provided by CrystalExplorer. Blue lines represent short intermolecular contacts below the sum of the van der Waals radii of the respective atoms. Colour chart: grey = C, white = H, red = O, and purple = N.

molecules, which are shifted with respect to each other (see Fig. 7C). Only OH···O (1.903 Å) and two types of CH···π interactions between pyridine–pyridine rings (2.898 Å) and pyridine–phenyl rings (2.826 Å) are involved in the formation of these chains (Fig. 7C). Additional CH···π and π···π interactions complete the 3D network. The parallel orientation of **Pic(St$_8$)$_3$** is obviously beneficial for the formation of mesophases with a larger temperature range (see Fig. 2), whereas the linear orientation of **Pic(Ap$_8$)$_3$** promotes faster crystallization.

Theoretical analysis of the crystal packing

To further understand the underlying mesogenic properties of the hydrogen-bonded assemblies, a packing analysis was performed to quantify the intramolecular interactions of the packing in the solid state. This packing cannot be directly correlated to the packing of the molecules in the mesogenic state, but can give, nonetheless, some insight into the predominant non-covalent interactions and therefore the liquid crystalline state.

The geometrical description of the crystal structures used above, in which we identified short intermolecular contacts and described them as contributors to the overall crystal packing, is common and easy to understand. However, this description gives only an incomplete picture of the factors that govern the crystal packing and it is of little help to quantify the intermolecular interactions in our structures. We thus used a methodology which is based on the intermolecular perturbation theory developed by Spackman,[16] which is in turn based on the work of Gavezzotti,[17] and implemented in the CrystalExplorer program.[18] This methodology allows for direct and accurate quantification of the intermolecular interactions and recently provided us insight into the aggregation-induced-emission (AIE) behavior of a series of liquid crystalline aromatic thioethers,[19] and explanation of subtle differences in the LC behavior of supramolecular liquid crystals based on natural products. Details on the methodology are given in the ESI.† In order to analyze the non-covalent interactions in the solid state a reference molecule in the crystal structure was defined (see Fig. 8 and 9 for details) and molecular pairs (structure determinants) with surrounding molecules were investigated with respect to their intermolecular interactions. In this respect, we selected the six most significant pairs (Fig. 8 and 9). In each structure determinant, the interaction energies are calculated and split into the individual contributions of electrostatics, polarization, dispersion and repulsion (ESI† Tables S2 and S3, for each individual contribution). Our structures are both disordered and we modelled them in the approximation that we are dealing with static disorder, so the disordered molecule can be in one conformation – or the other – in different cells. We present here the results for the most populated conformer of each of the two structures, but the conclusions do not change if the other two (less populated) conformers are considered. The main contributors to the crystal packing of this assembly are the two OH···N$_{py}$ hydrogen bonds, which are formed by two **Ap$_8$**

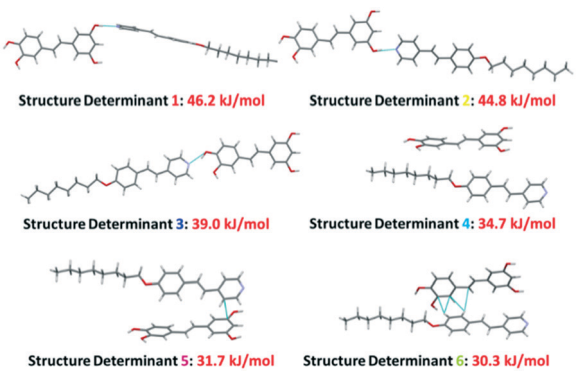

Fig. 9 Supramolecular hierarchy of the six most stabilizing interactions in the **Pic(St$_8$)$_3$** structure as provided by CrystalExplorer. Blue lines represent short intermolecular contacts below the sum of the van der Waals radii of the respective atoms. Colour chart: grey = C, white = H, red = O, and purple = N.

molecules and the "resorcinol" ring of the **Pic** molecule (44.9 and 44.2 kJ mol^{-1}, Fig. 8, structure determinants 1 and 2).

The third OH$\cdots$N$_{py}$ hydrogen bond ranks fourth in the interaction hierarchy with a reduced interaction energy (36.6 kJ mol^{-1}, Fig. 8, structure determinant 4) compared to the other two. We attributed this fact to the lower acidity of the hydroxy-protons in the "catechol" ring compared to those in the resorcinol ring of the **Pic** molecule.[20] Furthermore, due to the steric repulsion of the two vicinal OH groups, the weakest OH$\cdots$N$_{py}$ hydrogen bond has a slightly distorted geometry with an O–H$\cdots$N angle of 159°. This angle could be compared with the reference O–H$\cdots$N angle of 176° present in the "ideal" phenol–pyridine complex.[21] Interestingly, the remaining hydroxy-group, which does not interact with the pyridine rings of the **Ap$_8$** molecules, is involved in hydrogen bonding with another hydroxy-group of a neighbouring **Pic** molecule (Fig. 8, structure determinant 6).

The hydrogen bonds of structure determinants 1, 2, 4 and 6 are dominated by electrostatics (Fig. 8 and 9 and ESI† Tables S2 and S3), as expected. Important contributions to the crystal packing are also given by structure determinants 3 and 5, which feature CH$_{alk}\cdots\pi$ interactions that are dispersive in nature (Fig. 8 and 9).

Similarly to the structure previously described, the OH$\cdots$N$_{py}$ hydrogen bonding encompassing structure determinants 1–3 dominates the overall interaction ranking. There are however important differences between the packing of **Pic(St$_8$)$_3$** (Fig. 9) and the packing of **Pic(Ap$_8$)$_3$** (Fig. 8), due to the fact that, in the present case, $\pi\cdots\pi$ edge-to-face and stacked interactions are much more important energetically (structure determinants 4–6). Although the packing of **Pic(St$_8$)$_3$** (even that of any assembly) in the solid state cannot be directly compared with that in the LC state, the increased relevance of $\pi\cdots\pi$ and stacked interactions is important to promote the LC behavior, as the LC phase might be suppressed, when these interactions are hindered or disrupted.[22]

Conclusions

In conclusion, we reported liquid crystalline assemblies based on three different stilbenoids and two chalconoids formed from hydrogen bonds with alkylated stilbazoles or azopyridines which were found to be photoresponsive. The obtained single crystals also proved the formation of the hydrogen-bonded assemblies and allowed us to quantify the intramolecular interactions. While we observe mainly nematic phases for the HBAs, the **Oxy(St$_8$)$_3$** complex also showed a smectic liquid crystalline phase, as confirmed by SAXS and WAXS measurements. Furthermore, it was found that **Res(Ap$_8$)$_3$** and **Iso(Ap$_8$)$_3$** complexes reveal similar mesomorphic behavior, which can be attributed to their identical hydroxy-substitution pattern leading to comparable supramolecular assemblies despite their connectivity. As a result of these observations, it is suggested that the type of connectivity in the HB donors (*e.g.* with or without additional carbonyl-groups) of the phenolic units is less important than the number and position of the hydroxy-groups, which is remarkable since intramolecular hydrogen bonds in the chalconoids are present and need to be broken upon HBA formation. This observation supports the current understanding that the prediction of properties such as the kinds and range of mesophases as well as melting points and transition temperatures remains a challenging task. We expect for future experimental studies that naturally occurring polyphenolic compounds will lead to a plethora of novel liquid-crystalline complexes with different physical and chemical properties, helping to predict mesomorphism of supramolecular hydrogen-bonded complexes.

Conflicts of interest

There are no conflicts to declare.

Acknowledgements

Jun.-Prof. Jens Voskuhl acknowledges the Center for Nanointegration (CENIDE) for financial support. Jun.-Prof. Michael Giese is thankful for generous financial support from the Professor Werdelmann Foundation. Ass. Prof. Marco Saccone acknowledges PON R&I 2014–2020 – AIM (Attraction and International Mobility), project AIM 1813040 for financial support.

Notes and references

1 T. Beghyn, R. Deprez-Poulain, N. Willand, B. Folleas and B. Deprez, *Chem. Biol. Drug Des.*, 2008, **72**, 3–15.
2 Y. Liu, K. He, G. Chen, W. R. Leow and X. Chen, *Chem. Rev.*, 2017, **117**, 12893–12941.
3 A. Kashirina, Y. Yao, Y. Liu and J. Leng, *Biomater. Sci.*, 2019, **7**, 3961–3983.
4 (*a*) K. Rajan, J. K. Mann, E. English, D. P. Harper, D. J. Carrier, T. G. Rials, N. Labbé and S. C. Chmely, *Biomacromolecules*, 2018, **19**, 2665–2672; (*b*) K. J. De France, T. Hoare and E. D. Cranston, *Chem. Mater.*, 2017, **29**, 4609–4631.
5 G. Jutz and A. Böker, *Polymer*, 2011, **52**, 211–232.
6 M. Mitov, *ChemPhysChem*, 2014, **15**, 1245–1250.
7 P. Kirsch and M. Bremer, *Angew. Chem., Int. Ed.*, 2000, **39**, 4216–4235.
8 (*a*) H. Wang, H. K. Bisoyi, L. Wang, A. M. Urbas, T. J. Bunning and Q. Li, *Angew. Chem., Int. Ed.*, 2018, **57**, 1627–1631; (*b*) M. Saccone, M. Spengler, M. Pfletscher, K. Kuntze, M. Virkki, C. Wölper, R. Gehrke, G. Jansen, P. Metrangolo, A. Priimagi and M. Giese, *Chem. Mater.*, 2019, **31**, 462–470.
9 (*a*) M. Pfletscher, C. Wölper, J. S. Gutmann, M. Mezger and M. Giese, *Chem. Commun.*, 2016, **52**, 8549–8552; (*b*) M. Pfletscher, S. Hölscher, C. Wölper, M. Mezger and M. Giese, *Chem. Mater.*, 2017, **29**, 8462–8471; (*c*) M. Saccone, K. Kuntze, Z. Ahmed, A. Siiskonen, M. Giese and A. Priimagi, *J. Mater. Chem. C*, 2018, **6**, 9958–9963; (*d*) R. Y. Dong, C. A.

Michal, M. Saccone, M. Spengler, C. Wölper and M. Giese, *Chem. Phys. Lett.*, 2018, **710**, 39–44; (*e*) M. Saccone, M. Pfletscher, E. Dautzenberg, R. Y. Dong, C. A. Michal and M. Giese, *J. Mater. Chem. C*, 2019, **7**, 3150–3153.

10 M. Blanke, J. Balszuweit, M. Saccone, C. Wölper, D. Doblas Jiménez, M. Mezger, J. Voskuhl and M. Giese, *Chem. Commun.*, 2020, **56**, 1105–1108.

11 M. Saccone, M. Pfletscher, S. Kather, C. Wölper, C. Daniliuc, M. Mezger and M. Giese, *J. Mater. Chem. C*, 2019, **7**, 8643–8648.

12 (*a*) Y. Chen, H. Yu, L. Zhang, H. Yang and Y. Lu, *Chem. Commun.*, 2014, **50**, 9647–9649; (*b*) L. J. McAllister, C. Präsang, J. P. W. Wong, R. J. Thatcher, A. C. Whitwood, B. Donnio, P. O'Brien, P. B. Karadakov and D. W. Bruce, *Chem. Commun.*, 2013, **49**, 3946–3948; (*c*) M. Pfletscher, M. Mezger and M. Giese, *Soft Matter*, 2018, **14**, 6214–6221.

13 M. Rossi, F. Caruso, C. Opazo and J. Salciccioli, *J. Agric. Food Chem.*, 2008, **56**, 10557–10566.

14 S. Norio, U. Katsuhiko and S. Yoshio, *Bull. Chem. Soc. Jpn.*, 1972, **45**, 2274–2277.

15 M. Rossi, F. Caruso, E. J. Crespi, J. Z. Pedersen, G. Nakano, M. Duong, C. McKee, S. Lee, M. Jiwrajka, C. Caldwell, F. Baffour, D. A. Karlin, G. Lidoff, S. Leone, V. Balducci, J. Miler and S. Incerpi, *Biochimie*, 2013, **95**, 1954–1963.

16 M. J. Turner, S. Grabowsky, D. Jayatilaka and M. A. Spackman, *J. Phys. Chem. Lett.*, 2014, **5**, 4249–4255.

17 (*a*) A. Gavezzotti, *J. Phys. Chem. B*, 2002, **106**, 4145–4154; (*b*) A. Gavezzotti, *J. Phys. Chem. B*, 2003, **107**, 2344–2353.

18 J. J. M. M. J. Turner, S. K. Wolff, D. J. Grimwood, P. R. Spackman, D. Jayatilaka and M. A. Spackman, *CrystalExplorer17 (2017)*, University of Western Australia, 2017, http://hirshfeldsurface.net.

19 (*a*) S. Riebe, M. Saccone, J. Stelzer, A. Sowa, C. Wölper, K. Soloviova, C. A. Strassert, M. Giese and J. Voskuhl, *Chem. – Asian J.*, 2019, **14**, 814–820; (*b*) M. Saccone, S. Riebe, J. Stelzer, C. Wölper, C. G. Daniliuc, J. Voskuhl and M. Giese, *CrystEngComm*, 2019, **21**, 3097–3105; (*c*) M. Saccone, M. Blanke, C. G. Daniliuc, H. Rekola, J. Stelzer, A. Priimagi, J. Voskuhl and M. Giese, *ACS Mater. Lett.*, 2019, **1**, 589–593.

20 E. P. Serjeant and B. Dempsey, *Ionisation Constants of Organic Acids in Aqueous Solution*, Pergamon Press, 1979, p. 161.

21 T. Steiner, I. Majerz and C. C. Wilson, *Angew. Chem., Int. Ed.*, 2001, **40**, 2651–2654.

22 J. W. Steed and P. A. Gale, *Liquid crystals formed from specific supramolecular interactions*, John Wiley & Sons, Ltd, New York, 2012, pp. 3493–3515.